Fabrication of a microfluidic device for probiotic drug's dosage screening: Precision Medicine for Breast Cancer Treatment

Ali Salehi [a,b,1], Parvaneh Naserzadeh [c,1], Parastoo Tarighi [d], Elham Afjeh-Dana [a], Masoud Akhshik [e,f], Amir Jafari [b], Pooyan Mackvandi [b,g], Behnaz Ashtari [a,b,h,**], Masoud Mozafari [i,*]

[a] Radiation Biology Research Centre, Iran University of Medical Sciences, Tehran, Iran
[b] Department of Medical Nanotechnology, Faculty of Advanced Technologies in Medicine, Iran University of Medical Sciences. Tehran, Iran
[c] Endocrine Research Center, Institute of Endocrinology and Metabolism, Iran University of Medical Sciences, Tehran, Iran
[d] Department of Medical Biotechnology, Faculty of Allied Medicine, Iran University of Medical Sciences. Tehran, Iran
[e] Centre for Biocomposites and Biomaterials Processing. University of Toronto, Canada
[f] EPICentre, University of Windsor, Canada
[g] Centre for Materials Interfaces, Istituto Italiano di Tecnologia, viale Rinaldo Piaggio 34, Pontedera, 56025 Pisa, Italy
[h] Cellular and Molecular Research Center, Iran University of Medical Sciences, Tehran, Iran
[i] Research Unit of Medical Imaging, Physics and Technology, Faculty of Medicine, University of Oulu, Oulu, Finland

ARTICLE INFO

ABSTRACT

Breast cancer is the most common cancer in women; it has been affecting the lives of millions each year globally and microfluidic devices seem to be a promising method for the future advancements in this field. This research uses a dynamic cell culture condition in a microfluidic concentration gradient device, helping us to assess breast anticancer activities of probiotic strains against MCF-7 cells. It has been shown that MCF-7 cells could grow and proliferate for at least 24 h; however, a specific concentration of probiotic supernatant could induce more cell death signaling population after 48 h. One of our key findings was that our evaluated optimum dose (7.8 mg/L) was less than the conventional static cell culture treatment dose (12 mg/L). To determine the most effective dose over time and the percentage of apoptosis versus necrosis, flowcytometric assessment was performed. Exposing the MCF-7 cells to probiotic supernatant after 6, 24 and 48 h, confirmed that the apoptotic and necrotic cell death signaling were concentration and time dependent. We have shown a case that these types of microfluidics platforms performing dynamic cell culture could be beneficial in personalized medicine and cancer therapy.

Introduction

One of the most important and frequent types of cancer is breast cancer. It is responsible for the death of 40,000 each year globally [1,2]. Even with all the advancements in technology, the mainstream treatment is still removing the tumor via surgery and a few sessions of chemotherapy [3]. The sad truth about chemotherapy is that because of the toxicity of these treatments, the host will suffer as well as the tumor [4]. It should be noted that by using modern methods which help to early detection of tumors and cancer cells in the early stages, the chance for successful treatment has increased [5,6]. To enhance the success of

breast cancer treatment, modern diagnostic methods should be added at the beginning of tests, which is certainly a fact in developed countries. There are many biomarkers used in hormone-dependent and hormone-independent tumors such as pSTAT3 and LDH. Today, LDH is widely used for the routine diagnosis of many tumors, including breast cancer as a screening test [7–9]. The discovery of the next generation of treatments with fewer side effects is crucial in cancer therapy [10–13].

Probiotic has been used as suitable vessel for drug and active biomolecule delivery [14,15]. These known bacteria have shown an effective ability in fighting cancers and cancer therapy. They can also stimulate B and T cells in the immune system and guide them through

Peyer's patches to control mucosal sites like mammary glands [16]. Probiotic has been used as dietary supplement to improve human and animal health [17]. These bacteria can secrete different metabolites that protect gastrointestinal epithelial cells; they can regulate the immune system, and induce apoptosis. Probiotics also know for effects such as anti-inflammatory, anti-proliferative, anti-oxidative, and anti-mutagenic [18].

One of the most important steps in measuring the chemotherapies' effectiveness is *in vitro* drug sensitivity test [19]. This step helps to personalize the treatment by choosing the right drug and appropriate dose before starting the treatment for each individual [20]. *In vitro* studies need cell culture and this enables us to do some clinical science and biotechnology research [21]. There is a direct link between cellular level and animal experience in drug testing, which will help us to rapidly screen toxic or unusable drugs [22]. In recent years, cell culture has been about high-throughput cell-based assays which greatly contributed to our knowledge of cell biology [23,24]. With all the greatness, conventional cell culture has its cons. Some of the main drawbacks include the absence of predictiveness and not being like a real cell environment.

Microfluidic systems have been proven as a critical tool in cancer studies [25–28]. This technique lays out a new foundation in our current knowledge of cell biology. Owing to their excellent flow controls, microfluidics platforms are used for the creation of microdevices with the biochemical and physical environment of natural cells. These devices can control cell culture conditions in the physicochemical mimetic condition of the body, which makes them potentially a great tool in cell biology research [29–32]. The fact that these devices can manipulate a very low volume of fluids through micron-sized channels establishes the new biological design and experimental methods [33].

There are studies on the application of microfluidic concentration gradient devices in biological and clinical issues [34,35]. These systems are generally a web of channels that generate a gradient of different concentrations of a drug in cell culture chambers. There is even an interesting study of the interaction of carbon dots and yeast cells using these gradient systems [36].

One of the best methods to build these microfluidics platforms is soft lithography using PDMS as mentioned elsewhere [33,37]. In this study, we used the mentioned technique to mold our micrometric system made of PDMS from the hard substrate silicon wafer and plexiglas's. Then we used the 3 types of probiotic bacteria, namely Lactobacillus acidophilus, lactobacillus casei, bifidobacterium bifidum, which will give us different concentrations in our device. After confirming the growth of the seeded MCF-7 breast cancer cell line, different concentrations of probiotics were exposed to these cells and the most anti-cancerous concentration was identified.

Experimental section

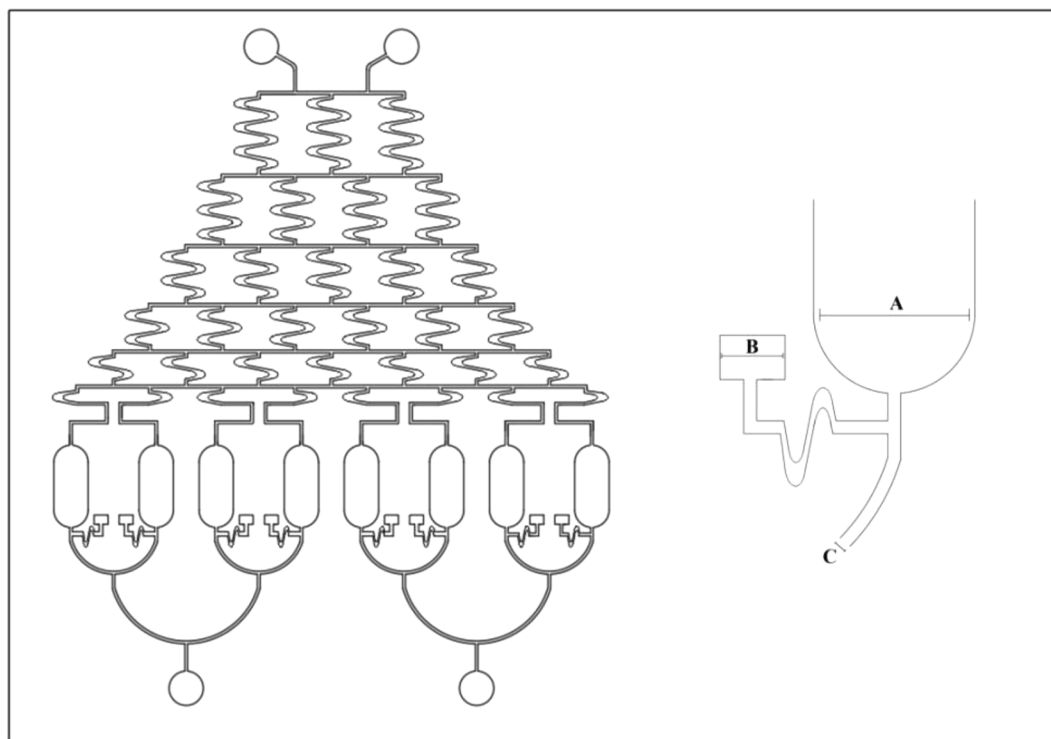### Microfluidic master designing

We have used AutoCAD 2017 (Autodesk Inc., California, and USA) to design the pattern for our system [38]. Simply our device contains eight cell-culture chambers, 2 inlet cylinders and 1 outlet and a network of channels which will create a concentration web and transports media between the inlets and outlet through the cell-culture chamber (Fig. 1).

Computational modeling

For the modeling of the computational fluid dynamics (CFD), we have used COMSOL Multiphysics 5.3a software (COMSOL Inc., Massachusetts USA) [39]. This software helped us to predict the Reynolds number inside our system and provide us with the velocity field evaluation.

Microfluidic device fabrication

As it was mentioned, we used PDMS to fabricate our concentration gradient microfluidic device via soft lithography [37]. To make this device we transferred the designed pattern to the mask by using a high-resolution printer. The pattern was then transferred to the photo-resist negative SU-8 substrate by the standard photolithography technique. Then we mixed the PDMS and elastomer (10:1) to make PDMS

Fig. 1. The microfluidic master design using a 2017 AutoCAD (AutoDesk Inc. California USA). Details of gradient generating system shown on the right. (A: 550 μm, B: 230 μm, C: 2900 μm, D: 800 μm).

cast using the SU-8 as a mold. The next step was degassing for 20 min with a desiccator followed by baking at 85 °c on a hot plate (2 h). The PDMS chips were then cut by a precision cutting knife followed by punching the connection ports with a 1 mm puncher. To bond PDMS cast to glass, we have used oxygen plasma activation. We used 1 mm PTEE tubes to connect the syringe pump to the ports to form the final microfluidic device ready to be used.

Microfluidic device preparation for cell culture

Like every other cell culture, we have sterilized the components and microfluidic device first. To further enhance cell adherence, we have coated the device's cell chambers with%0.2 collagen type IV at room temperature for 30 min. After coating, the unattached collagen was rinsed with distilled water followed by blocking with%2 BSA (4°c overnight). After blocking, the syringe pump and inlet were connected by PTTE tube and this make the device ready for the cell culture.

Cell culture

Human breast cancer (MCF-7) cell line (from The Institute Pasteur) was cultivated in standard RPMI 1640 medium with 10% (w/v) Gibco (TM)'s fetal bovine serum (FBS) (from Thermo Fisher Scientific Inc., USA) and 1% Invitrogen (TM)'s penicillin/streptomycin (from Thermo Fisher Scientific Inc., USA). Using a standard T25 flask in the incubator (37°c, 5% CO_2) the medium was replaced every 48 h. MCF-7 cells were grown to 80–90% confluency and harvested with Trypsin-EDTA (0.05% w/v) (Sigma, USA) [40].

After the preparation of MCF-7 cells and human fibroblast (HGF-1) (10^6 cells/mL) as a normal cell, these cells were seeded into the cell chambers under a sterile condition with 0.2% collagen coating. After injection, to supply fresh nutrients, a fresh culture media was supplied to the concentration gradient networks with programmable syringe pumps. Besides monitoring the cell proliferation with an optical microscope every day (MODEL: ELWD 0.3 T1 SCP, Nikon, JAPAN), we have also collected the UV–visible imaging of the MCF-7 and HGF-1 cells in the chambers via an inverted microscope. Then, we analyzed the images, merged them, and the cells in each chamber were counted by ImageJ software (from the National Institutes of Health (NIH), USA).

Probiotic supernatant preparation

Probiotic bacteria (L. acidophilus, lactobacillus casei, bifidobacterium bifidum) were cultured anaerobically in De Man, Rogosa, and Sharp MRS broth (Quelab laboratories Inc., Quebec, Canada) at 37°c for 48 h. While still in the stationary phase, the solution was centrifuged in 1000 g for 15 min at 4 °c. The probiotic supernatant was collected and then measured in a spectrophotometer (Pharmacia Biotech Inc., USA) at OD600. This supernatant was freeze-dried and kept for further applications [41].

Cell viability

Performing a standard MTT assay on 12 and 24 h the viability of HGF-1 and MCF-7 was assessed. To perform this assay, concentrations of 2, 4, 8, and 16 mg/mL were tested in 48 well plates. Simply the samples were cultivated in a blend of the MTT and serum-free medium for 3 h.

Then we used an ELISA reader (570 nm) to measure the absorbance of generated formazan crystals after dissolving in dimethyl sulfoxide (DMSO). For each concentration, the test was performed in three replicas [42,43].

We have used flow cytometry sorting, with the flowing software-2-5-1 and 488 nm Argon ion LASER detectors to collect cells. Simply the crude cells dissolved in PBS (0.5 ml) and aliquoted into 100 μL samples. Then these samples were fed into the BD flow cytometry tube. Then we used BD Biosciences FACS Calibur (TM) flow cytometer to examine the cells by fluorescence and light scattering for a minimum of 10,000

counts for each sample. To exclude cell debris and clamp, we used forward/side scatter techniques (FSC/SSC, in which FSC refers to cell morphology and SSC refers to cell granularity).

Toxicity assessment using flow cytometry

There are specific tests for the evaluation of apoptosis [44,45]. Here, we have used flow cytometry to evaluate cell toxicity [45]. MCF-7 cell line was treated with a gradient of concentration of probiotic supernatant (0, 0.18, 1.31, 3.62, 7.81, 10.81, 11.81, 12 mg/mL). Then, the percentage of apoptosis vs. necrosis was calculated for three concentrations (3.6, 7.81 and 10.81 mg/mL) at 6, 24 and 48 h. We have used the Annexin V-FITC Apoptosis Detection kit (Sigma Inc., USA) to perform double staining with fluorescein isothiocyanate and propidium iodide (PI). The final concentration of FITC-Annexin was 5 μM and the cells were incubated in a dark for 15 min afterward. After 15 min these cells were rinsed with PBS, Centrifuged and resuspended in a binding solution. Just before performing the flow cytometric analysis, we added 10 μM PI (solved in the binding solution) to the samples. Finally, the fluorescence signals from Annexin V and PI were analyzed in FL1 and FL2 channels.

Reactive oxygen species assay

The MCF-7 cells (which were in probiotic concentrations of 3.6, 7.8 and 10.81 mg/mL) were incubated in the respiration culture media. Taking a sample from these cells, we added 2,7-dichlorofluorescein diacetate (DCFH-DA) to a final concentration of 10 mM in the cells. These samples were incubated for 6, 24, 48 h [46]. Then we used our flow cytometer to find the optimum concentration which provoked ROS generation in cells. We have performed this test in the FL1 channel with a 530 nm band pass filter. Each reported number here is based on the mean intensity of 10,000 fluorescence counts.

Results

Modeling, fabrication and characterization of the microfluidic device

Our concentration gradient microfluidic device was manufactured by standard soft lithography and to increase the cell adhesion we coated the device's interiors with 0.2% collagen type IV before cell injection. Then, to supply fresh nutrients, after solving the convection-diffusion equation and simulating the fluid field, a fresh culture media was supplied to the concentration gradient networks with programmable syringe pumps at the constant flow rate of 0.1 mL/h with no-slip boundary. Then imaging of the MCF7 cell proliferation was collected via an inverted microscope every day (Fig. 2)

Cell viability

As mentioned, we have used the MTT assay to determine the cell viability with different concentrations of the three kinds of probiotic bacteria mix. We also utilize the cell viability as the measure for cell functionality on HGF-1 (Fig. 3) and MCF-7 (Fig. 4) cells on 6 and 24 h of the incubation with probiotic mixes a,b,c,d,e,f (1, 4, 8, 12, 16 mg/mL) concentration.

Drug treatment evaluation

Fig. 5 shows the MCF-7 cells, 24 h after seeding in the microfluidic device cell chambers. These cells were exposed to gradient concentrations of probiotics (0, 0.18, 1.31, 3.62, 7.81, 10.81, 11.81, 12 mg/mL).

ImageJ software analysis

For cell counting in the chamber of microfluidic device. We used the
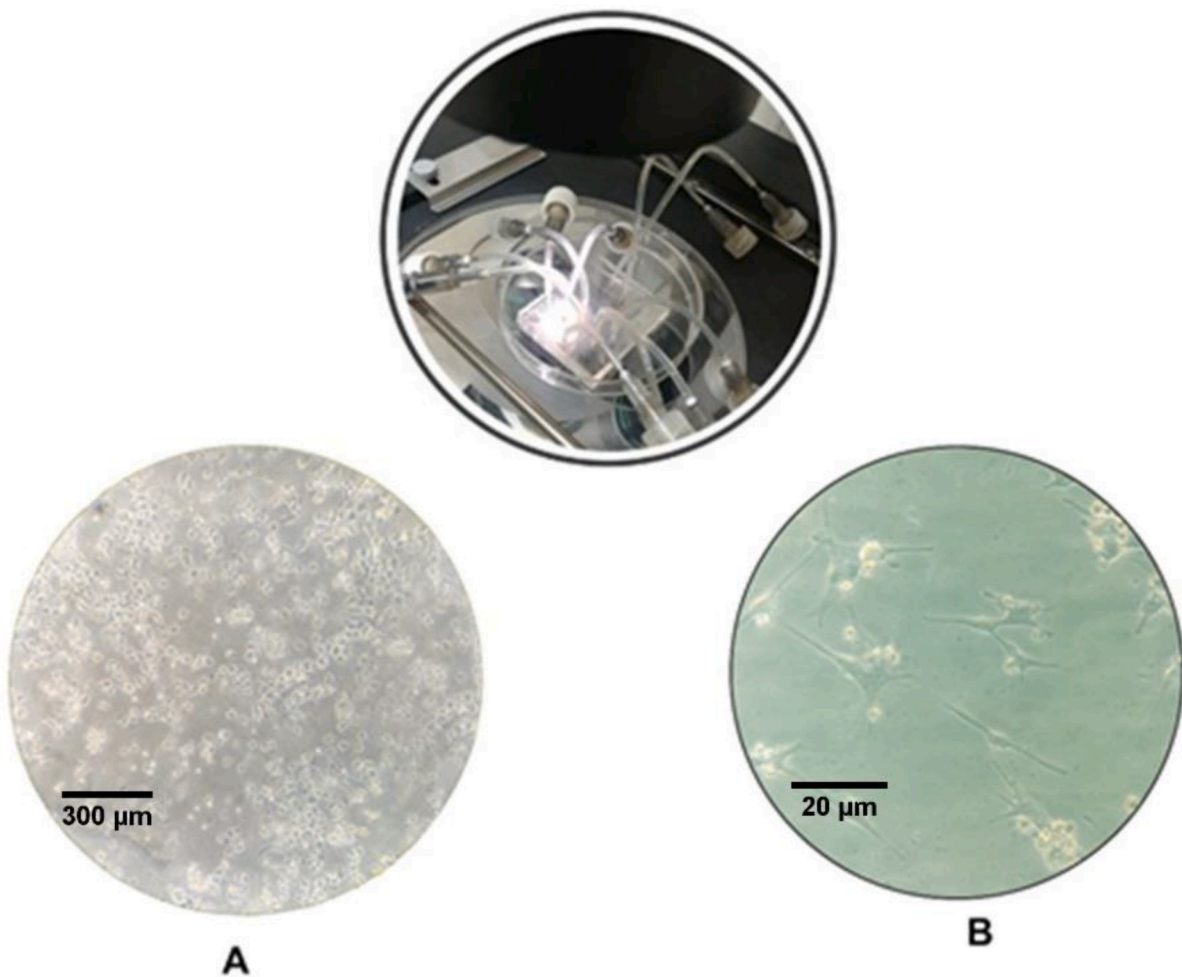
Fig. 2. An inverted microscopic image of the adherence of the MCF-7 cells in microfluidic cell chambers A) one day after cell injection using $a \times 10$ lens B) the same cell chamber after 3 days with $a \times 40$ lens.

image j software. Fig. 6 shows the cell counting after cell seeding and drug treatment in chamber 4 (7.81 mg/mL) at 24, 48 and 72 h.

ROS evaluation

In this study, The ROS formation assessment was performed for the probiotic concentrations of 3.62, 7.8 and 10.68 mg/mL after 6, 24 and 48 h at different concentrations and times. Fig. 7A &B demonstrated the results of ROS assessment.

Flow cytometry assessment

The apoptosis was quantified by the externalization of phosphatidylserine (PS) and Propidium iodide (PI) stains used as an indicator of membrane integrity for nuclear. The apoptosis/necrosis assessed by Annexin V/PI double staining at 6, 24, and 48 h (Fig. 8 and Table 1). Our results showed that by exposing MCF-7 cells to probiotic supernatant concentrations (3.6, 7.8 and 10.68 mg/mL) we can induce cell death signaling.

Discussion

In this study, we designed and manufactured a microfluidic device to assess the effectiveness of probiotics in breast cancer therapy. This platform was capable of creating a gradient of probiotic concentration exposed to the breast cell cancer line (MCF-7). One of the advantages of using the microfluidic system here was keeping the physicochemical environment similar to the human body. Microfluidic systems are one of the most effective techniques used in cancer therapy research [43].

Microfluidic systems have been used in several studies in cancer treatment.

For instance, using microfluidic devices demonstrated that the optimal concentration of curcumin for sensitizing prostate cancer PC3 cells is lower than the current TRAIL treatment and adjustments need to be taken into account for the clinical applications [47]. There is a study on breast cancer involving the microfluidic device. This device includes an upper and a lower microchannel which is separated by a semi-permeable membrane that imitates the 3D structures of the human mammary duct (HMD). This microdevice was employed to evaluate drug effectiveness on co-cultured breast tumor spheroids with HMD epithelial cells and mammary fibroblast cells. The upper microchannel offered the ductal lumen that allows the continuous flow of culture media which is essential for growing and preserving the mammary epithelial cells and DCIS spheroids on the upper side of the extracellular matrix membrane. This study proved that paclitaxel influences the size of DCIS and was able to restrain tumor cell proliferation and growth of DCIS in the tumor microenvironment [48]. So we designed one microfluidic device to evaluate the effectiveness of probiotics on MCF-7 breast cancer cells. Fig. 1 demonstrated the pattern of this microfluidic device that was designed by AutoCAD software. Cell adherence, proliferation, and viability in the studies showed that the microfluidic device is suitable for cell culture especially if coated with gelatin. Because of having many pores in PDMS, these devices are gas permeable and they can be used in an incubator and it is also transparent which makes them great
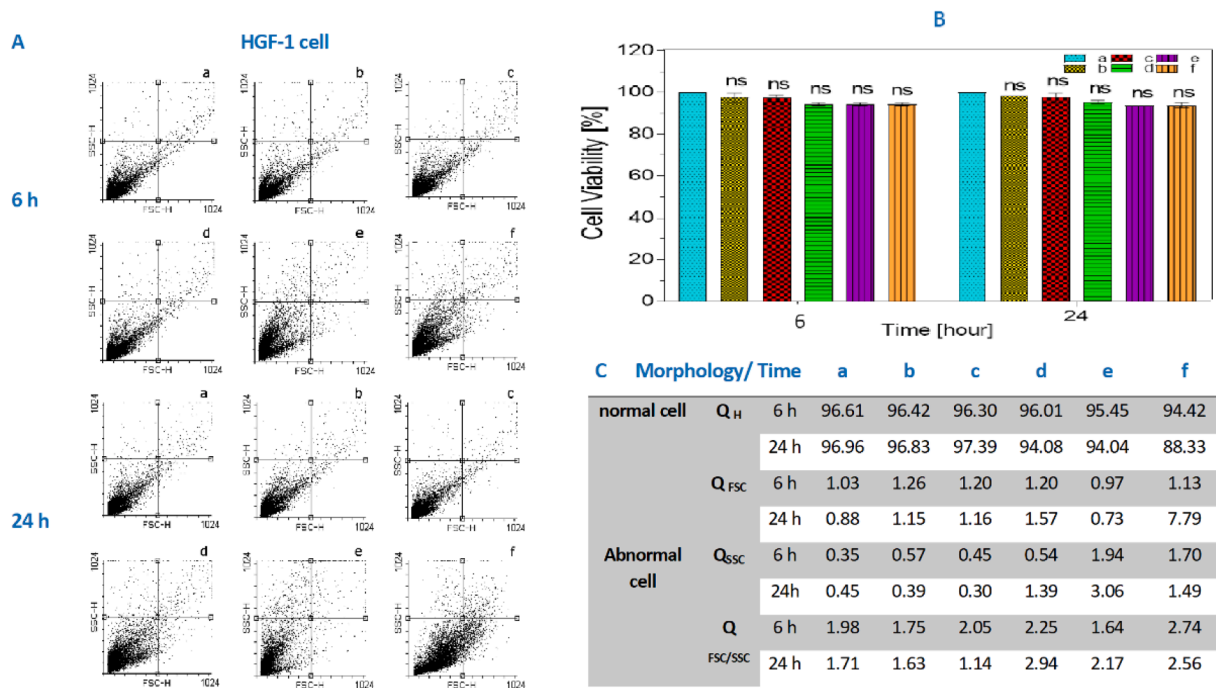
Fig. 3. (A) the cell count in HGF as it was mentioned cells was examined by flow cytometry. (B) Shows the MTT assay with different concentrations of probiotic bacteria after 12 and 24 h. As depicted in the chart, our probiotic supernatant did not affect the HGF-1 cells significantly in comparison to the control group. All the values are expressed as means ± SD (n = 3) and ns = not significant, compared with control group. Figures C show the cell count in HGF by QH, QFSC, QSSC and QFSC/SSC. (QH = quadrant Health population, QFSC=quadrant Forward side scatter population (shown cell had change shape), QSSC = quadrant Side scatter population (shown cell had change granulate)).
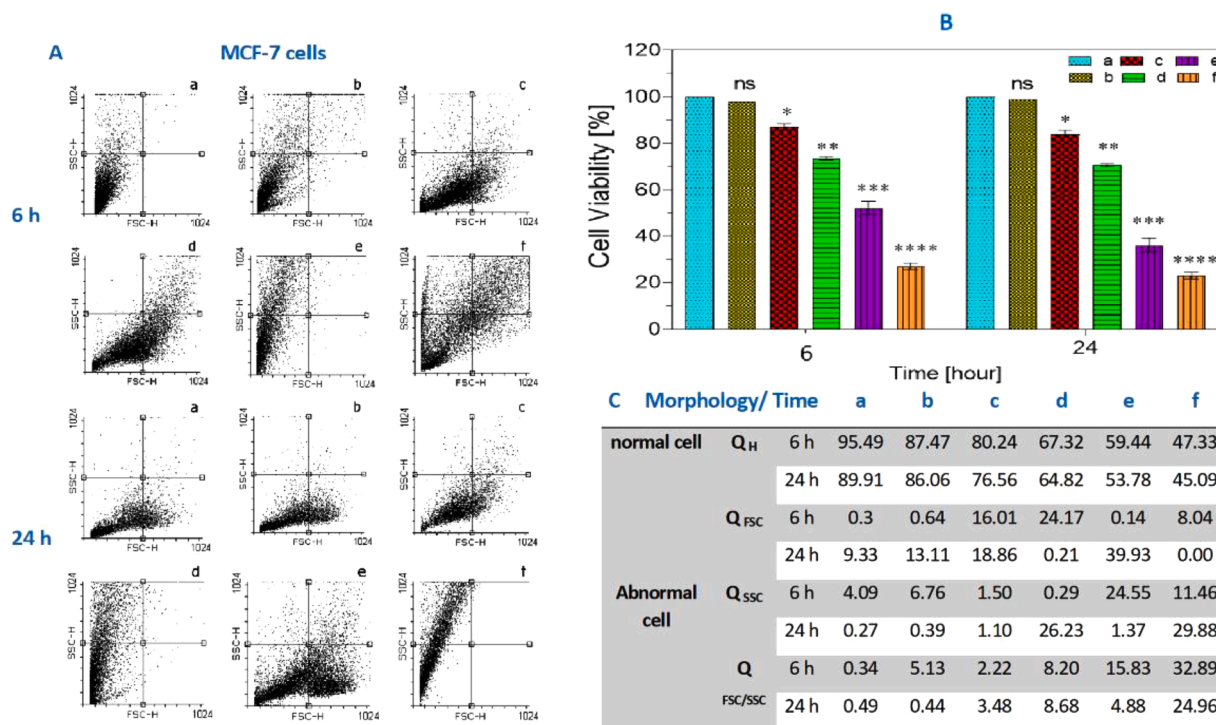
Fig. 4. (A) The cell count in MCF-7 as it was mentioned cells was examined by flow cytometry. (B) Shows that the probiotic supernatant kills approximately 50% of MCF-7 cells at 12 mg/mL. All the values are expressed as means ± SD (n = 3). ns = not significant, *$P < 0.05$, **$P < 0.01$, ***$P < 0.001$ and ****$P < 0.0001$ compared with control group. (C) the cell count in MCF-7 by QH, QFSC, QSSC and QFSC/SSC. (QH = quadrant Health population, QFSC = quadrant Forward side scatter population (shown cell had change shape), QSSC = quadrant Side scatter population (shown cell had change granulate)).
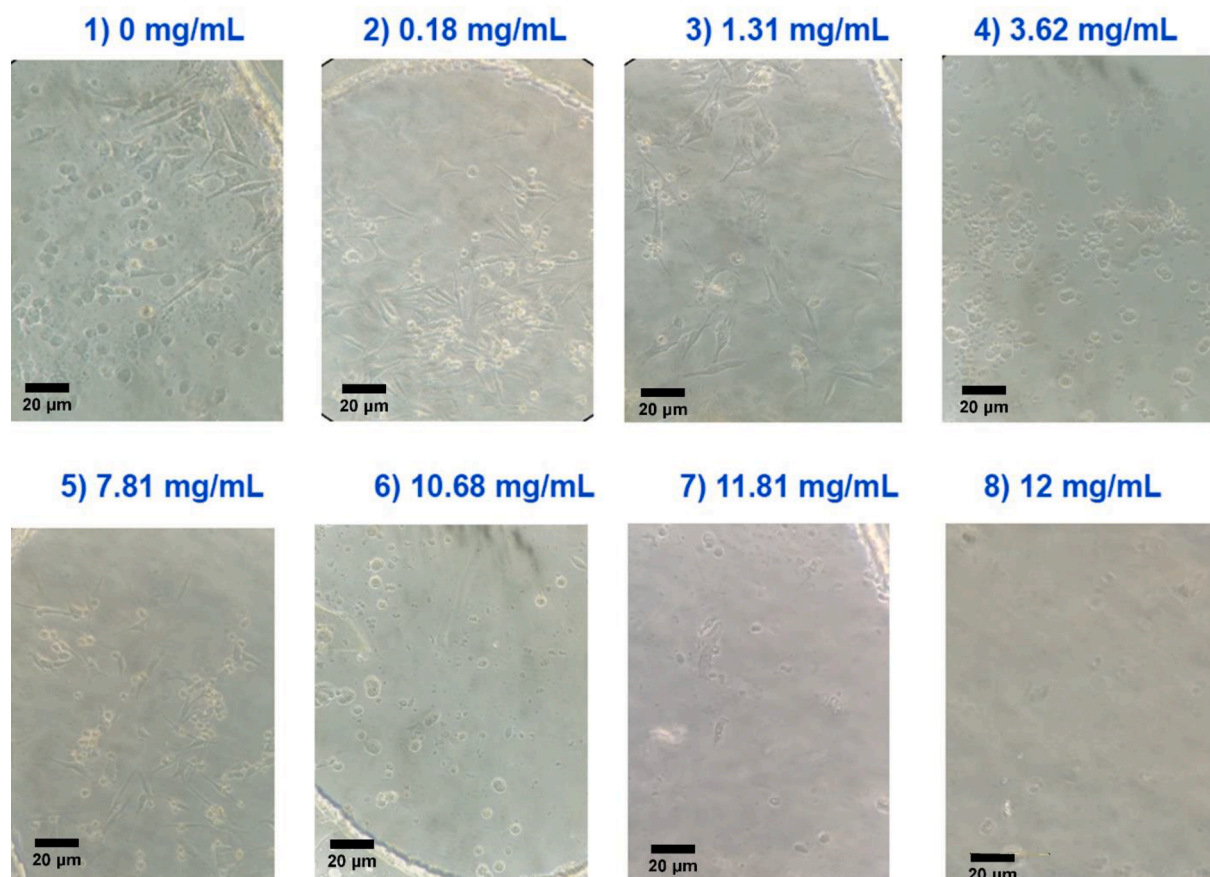
Fig. 5. The invert microscopic image of the cell culture chambers containing MFC-7 cells after 24 h × 20 lens. Each chamber has a different concentration of probiotic and the most effective chamber was chamber 4 with the concentration of 7.81 mg/mL. These data confirmed that the optimal probiotic supernatant concentration to kill more than 50% of cells was 7.81 mg/mL which was lower than the result from flow cytometry and MTT assay.

for imaging microscopy [49]. Therefore, our microfluidic device coated with 0.2% collagen. With the coating of 0.2% collagen, we were able to provide a great platform for breast cancer cells to adhere, proliferate and stay alive. Fig. 2 shows an imaging of the MCF-7 cell proliferation in the chambers via an inverted microscope that we have collected every day.

To evaluate the viability of HGF-1 and MCF-7 cells, the standard MTT assay at 12 and 24 h was performed. Fig. 3 shows the fact that HGF-1 cells' enzyme activity did not change significantly with the addition of probiotic mix concentrations up to 16 mg/mL in comparison with our control group. We were not able to detect IC_{50} value after 24 h of incubation. Fig. 4 shows that the MC-F cells remain alive up to 8 mg/mL in comparison to the control group. On the two higher concentrations (12 & 16 mg/mL) more than 50% of cells were not viable in 24 h. The ordinary cell treatment also agreed on 12 mg/mL as the IC50. While HGF-1 cell viability was over 80% of the population after 6 and 24 h of probiotic exposure (Fig. 3B), Most of the MCF-7 cells experienced a change in population shape (FSC>Count/population) with 8 mg/mL after 12 h (Fig. 4A, C). By increasing the probiotic concentration to 12 mg/mL more than 50% of cells have the changes in the granularity (SSC>Count/population) after 12 and 24 h (Fig 4), while HGF-1 Cell, we did not see any change in count/population (Fig. 3A, C). Many studies utilized MTT assay for evaluating HGF-1 and MCF-7 cell viability during the exposure to drugs or anti-cancer agents [50–52]. According to the comparison of the results obtained in our study with other studies, it can be confirmed that the results of cell viability using the MTT assay can be relied upon. Probiotics, in addition to their nutritional value, are an effective cancer treatment. Some of the probiotic strains can release bioactive metabolites which can prevent and/or inhibit the growth of breast tumors by stimulating an immune response [53]. For example, one study suggested

that potential probiotic strains (L. fermentum RM28 and E. faecium RM11) increased 21–29%, and 22–29% antiproliferation in colon cancer cells [54]. Also, Tiptiri-Kourpeti et al. indicated that L. casei ATCC 393 strain approximately 80% reduction in tumor volume of treated mice and regulated tumor-inhibitory, anti-proliferative and pro-apoptotic in colon cancer cells and [55]. These benefits are all added to the benefits of chronic intestinal diseases and autoimmune diseases [56–58]. Probiotics are shown to be effective in some types of human cancer such as colon cancer [54]. At the clinical stage, heat-killed probiotic strains, like lactic acid bacteria and Bifidobacterium, have been used for intestinal diseases [55,59], allergic respiratory [60], and dermatitis diseases [61]. Using heat-killed bacteria, compared to live microorganisms, can provide disrupted cells and release the bacterial components. This is similar to the *in vivo* and the physiological conditions of the gut lumen and outer mucus layer. These sorts of microorganisms can be easily and safely used for many diseases [62]. One of the most widely used breast cancer cell lines, which have been employed for many years by several researchers, is MCF-7, it is also the go-to cell line for breast cancer drug research [63].

For these reasons, we also used probiotics in this study. For this purpose, cancer cells were exposed to a gradual concentration of probiotics (0, 0.18, 1.31, 3.62, 7.81, 10.81, 11.81, 12 mg/mL) 24 h after seeding in a microfluidic device. As with the results of other studies on the use of probiotics as an anti-cancer agent, the inverted microscopy analysis by Image J software confirmed that our desired drug can be lethal at concentrations as low as 7.81 mg/mL (Fig. 5). Also Fig. 6 which is related to the cell counting after cell seeding and drug treatment in chamber 4 (7.81 mg/mL) at 24, 48, and 72 h, confirmed that the cell population decreased in chamber 4 by more than 50%.
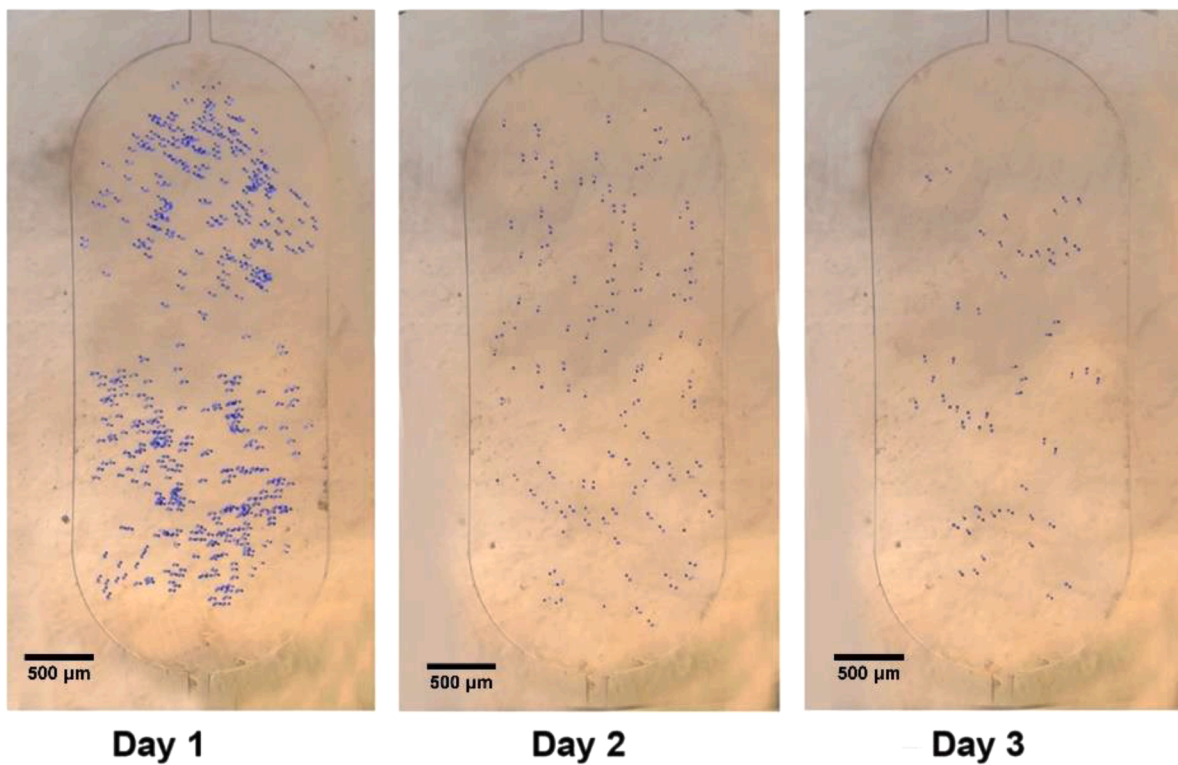
Fig. 6. The chamber 4 Cell counting using ImageJ software × 4 lens. The counting results revealed that one day after treatment, the numbers of MCF-7 cells were decreased significantly.
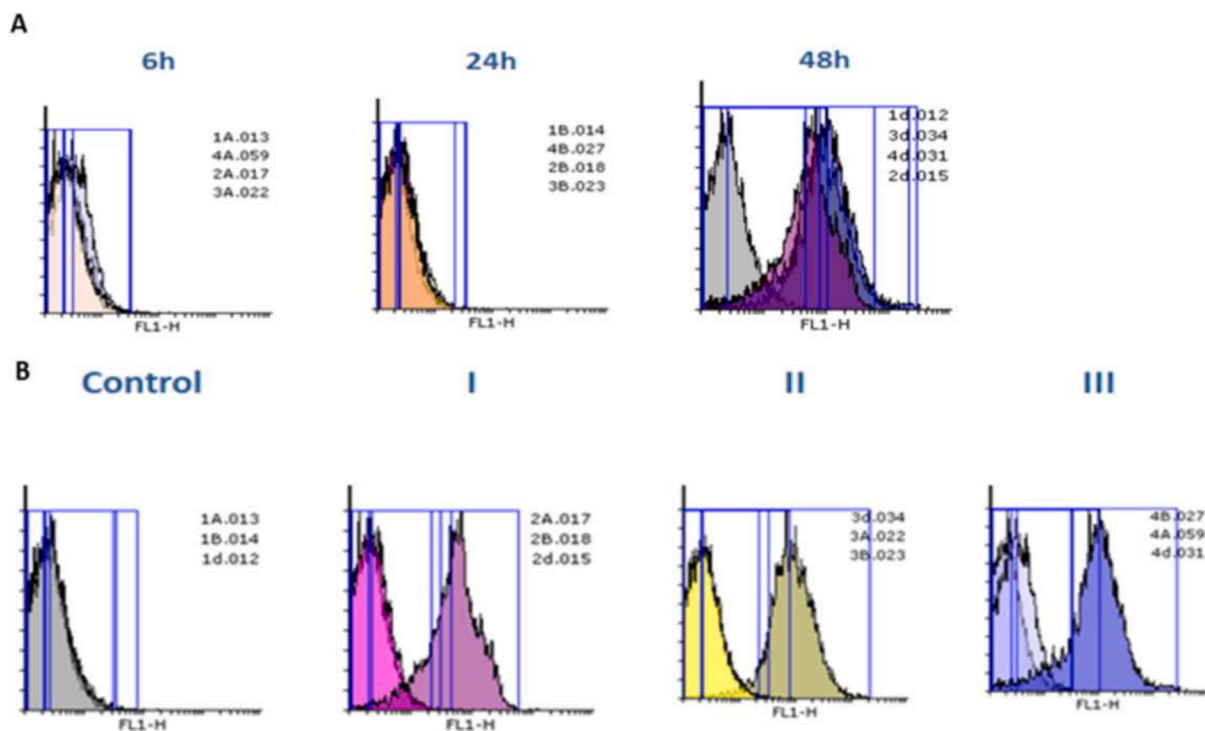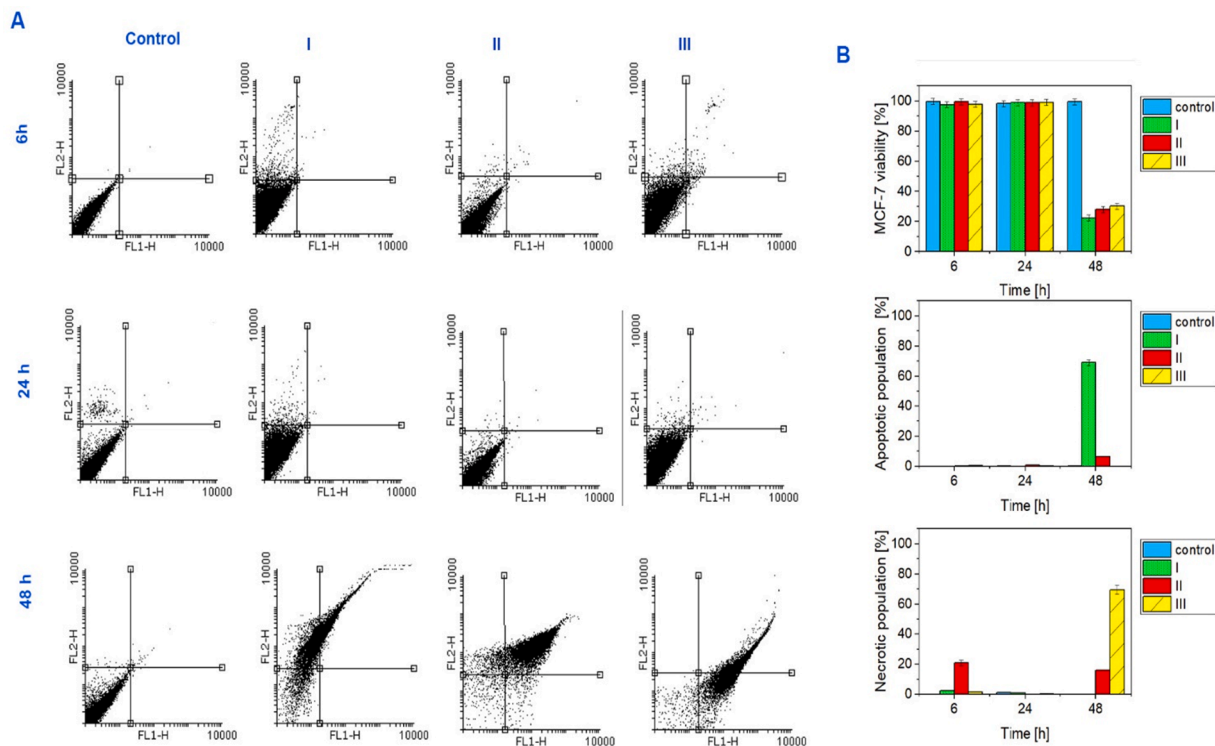

Fig. 7. The formation of the ROS at different concentrations of probiotic supernatant (I, II, III are 3.62, 7.8 and 10.68 mg/mL, respectively) and time (6, 24, and 48 h, respiratory). The results of constant concentration (A) and constant time (B) in MCF-7 cells are shown.

As far as we know the mitochondria are a critical organelle in cell death and ROS plays an important role in the cytotoxicity processes. In detail, ROS increases the mitochondrial permeability transition (MPT). The process of pore opening is caused by the oxidation of thiol (S-S) groups that play a key role in the enhancement of the peroxidation of the lipid cell membrane and mitochondrial membrane potential collapse (MMP). This collapse leads to the opening of the MPT pores and the release of cytochrome from the mitochondrial intermembrane space into

Fig. 8. The cells population after 6, 24 and 48 h for exposure to different concentrations of probiotic supernatant (I, II, III are 3.62, 7.8 and 10.68 mg/mL, respectively). As you can see MCF-7 cells stay alive after exposure to probiotic supernatant for all concentrations after 6 and 24 h, whereas the viability of MCF-7 cells after 48 h decreased and showed dose dependency.

Table 1

shows the cells percentage population after 6, 24 and 48 h for exposure to different concentrations of probiotic supernatant (I, II, III are 3.62, 7.8 and 10.68 mg/mL, respectively). As you can see MCF-7 cells stay alive after exposure to probiotic supernatant for all concentrations after 6 and 24 h, whereas the viability of MCF-7 cells after 48 h decreased and showed dose concentration and time dependency compared with control group at each time of concentration. All the values are expressed as percentage. ns = not significant, $*P < 0.05$, $**P < 0.01$, $***P < 0.001$ and $****P < 0.0001$ compared with control group.

Apoptosis/Necrosis assay%					
Cell-Time/ (mg/ml)	Concentration	Control	I	II	III
Live cell	**6h**	99.72	97.45 ns	99.53ns	97.77**
	24h	98.35	98.89 ns	98.95ns	99.07**
	48h	99.51	11.93***	28**	4.14****
Necrotic cell	**6h**	0.02	2.47*	21****	1.07*
	24h	1.25	0.93*	0.04****	0.45*
	48h	0.1	0.00*	16.25****	40.25****
Apoptotic cell	**6h**	0.16	0.00*	0.12*	0.43***
	24h	0.26	0.06***	0.97**	0.27**
	48h	0.19	42.16****	6.42**	0.01*

the cytoplasm which in turn activates the caspases family such as caspase-3 effectors, along with a decreased adenosine triphosphate nucleotide (ATP) will cause the cells to die [64,65]. In this study, The ROS formation assessment was performed for the probiotic (3.62 and 7.8, and 10.68 mg/mL concentrations) after 6, 24, and 48 h. The results show that There was no fluorescence intensity peak shift to the right in the constant concentration (I, II, and III are 3.62, 7.8, and 10.68 mg/mL, respectively), after 6 and 24 h. However, after 48 h we were able to detect a considerable ROS formation (Fig. 7A) and the right shift can be observed in all the concentrations rather than in the control group (0 mg/mL). Fig. 7B shows the analysis of constant time (6, 24, and 48 h) at different concentrations. Peak shifting at all concentrations (I, II, III are

3.62, 7.8, and 10.68 mg/mL, respectively) are detectable after 48 h in comparison with the control group. However, there is no significant right shifting after 6 and 24 h compared with the control group (0 mg/mL) in MCF-7 cells. From these diagrams, it can be concluded that the ROS formation caused by probiotics is independent of time and dose concentration. Similarly, in one study authors utilized ROS assessment for the evaluation of gold nanoparticles as an anticancer agent on MCF-7 death [66]. Also, other studies used ROS assay in breast cancer therapy research [67,68]. There are other examples of apoptosis induction via ROS formation caused by probiotics effects. One study indicated that L. acidophilus affects to release of cytokine, tumor growth rate, increased lymphocyte proliferation, and systemic immune responses against transformed cells [61]. Moreover, LA-EPS-20,079 oligosaccharides induced apoptotic and NF-κB inflammatory pathways in human colon cancer [62]. Lactobacilli-EPSs such as delbrueckii ssp and bulgaricus B3 activated level of glucose composition, cell proliferation and apoptosis factor in human colon cancer [63]. Also, Probiotic-derived ferrichrome induced apoptosis, which is mediated by the activation of c-jun N-terminal kinase (JNK) signaling pathway and probiotic-derived ferrichrome exerts a tumor-suppressive effect via the JNK signaling pathway [64]. Comparing our results and the results from other researches showed that the results obtained from ROS analysis could be confirmed.

To determine the most effective probiotic concentration, a flow cytometric assessment was performed and the percentage of apoptosis versus necrosis for MCF-7 cells was determined in exposure to different concentrations of probiotics over time. In the early stages of apoptosis, phosphatidylserine (PS) is translocated from the inner side of the plasma membrane to the outer layer. Annexin V is a calcium-dependent phospholipid-binding protein with a high affinity for PS. Therefore, it can be used as a sensitive probe to detect PS on the cell membrane and as a marker of apoptosis. Annexin V is a detector of apoptosis that stains membrane lipid phosphatidylserine. Propidium iodide (PI), which stains the nuclear, thus can be used as an indicator of membrane integrity and necrosis. We use these probes to gather information about the cells. Our

previous study showed that the balance between cell growth and apoptosis plays an important role in the treatment and disease progress [69,70]. As you can see in Fig. 8 and Table 0.1, live cell count in chambers after 6 h of exposure to the probiotic concentrations (0, 3.62, 7.8, and 10.68 mg/mL) was normal compared with the control group respectively. The necrotic cell counts and the apoptosis cell counts in the same order of chambers were measured and we showed minimal changes in population percentage compared with the control group. Similarly, at 24 h, live cell counts were changed compared with the control group. The necrotic cell counts and the apoptosis cell counts in the same order of chambers were measured and we showed a changed population percentage compared with the control group. Interestingly at 48 h, live cell counts decreased in media. The necrotic cell counts and the apoptosis cell counts in the same order were increased in media respectively (Fig. 8 and Table 0.1). Similarly, some studies utilized annexin V/PI analysis for evaluation of MCF-7 cells apoptosis and necrotic cells death [71–73]. For example, Yedjou et al. Researchers used annexin V/PI analysis to investigate the effect of Vernonia amygdalina (VA) leaf extracts as an anticancer agent on the apoptosis of MCF-7 cancer cells and also to examine necrotic cells. The results of this analysis showed that VA causes externalization of phosphatidylserine along with secondary necrotic cell death, which indicates cytotoxicity and apoptosis in MCF-7 cells [74]. The results obtained in the present research are similar to the results of previous studies on the toxicity of anticancer agents on breast cancer cells.

Our results confirmed that the apoptotic and necrotic cell death signaling depends on time and the concentration of the probiotic supernatant treatment. The optimal dose of probiotic supernatant treatment in our microfluidic system was 7.8 mg/ml which is less than the MTT assay results (12 mg/mL). As we know microfluidic systems can provide spaces similar to the internal body spaces and, they can be more accurate and sensitive (to the cellular level) than other conventional tools like flow cytometry and MTT assay. We were able to utilize a concentration-gradient microfluidic system to obtain the optimum dose of the drug which will result in personalized medicine.

Conclusions

In conclusion, due to some exclusive features of microfluidic systems, e.g. accurate and high throughput, inexpensive format, high capability for parallelization, precise measurement, and continuous exchange of cell culture medium, these systems have been applied increasingly in diagnosis and the treatment of various sorts of cancer diseases. In this study, to evaluate the optimum dose of our probiotic mixture (L. acidophilus, L. casei, Bifidobacterium bifidum) on the MCF-7 breast cancer cell line, We have injected different concentrations (0, 0.18, 1.31, 3.62, 7.81, 10.81, 11.81, 12 mg/mL) of the probiotic into the cell chambers in the gradient-generating microfluidic device. It was found that 7.8 mg/mL (IC$_{50}$) of the drug was able to significantly decrease the viability of MCF-7 cells. To compare we repeat the same experiment using a conventional cell culture flask; however, the optimum dose of probiotic supernatant to kill approximately 50% of cells in MTT assay using an ordinary cell treatment was 12 mg/mL which means the microfluidic system can give us more sensitive and accurate results. This could be the first step toward finding an optimum dose of treatment for cancer treatment for every person and avoiding the drastic side effects.

CRediT authorship contribution statement

Ali Salehi: Writing – original draft, Conceptualization, Methodology, Investigation. **Parvaneh Naserzadeh:** Writing – original draft, Methodology. **Parastoo Tarighi:** Writing – original draft, Conceptualization. **Elham Afjeh-Dana:** Writing – original draft, Investigation. **Masoud Akhshik:** Writing – original draft, Software, Validation. **Amir Jafari:** Methodology, Visualization. **Pooyan Mackvandi:** Writing – original draft. **Behnaz Ashtari:** Conceptualization, Supervision, Writing

– review & editing. **Masoud Mozafari:** Conceptualization, Supervision, Writing – review & editing.

Declaration of Competing Interest

The authors declare that they have no known competing financial interests or personal relationships that could have appeared to influence the work reported in this paper.

Acknowledgments

References

[1] S. Bhatia, et al., Interrogation of phenotypic plasticity between epithelial and mesenchymal states in breast cancer, J. Clin. Med. 8 (6) (2019) 893.

[2] C. Giordano, et al., Leptin modulates exosome biogenesis in breast cancer cells: an additional mechanism in cell-to-cell communication, J. Clin. Med. 8 (7) (2019) 1027.

[3] M. Casiraghi, et al., Surgery for small cell lung cancer: when and how, Lung Cancer 152 (2021) 71–77.

[4] A.M. Tavener, M.C. Phelps, R.L. Daniels, Anthracycline-induced cytotoxicity in the GL261 glioma model system, Mol. Biol. Rep. 48 (1) (2021) 1017–1023.

[5] A. Khamparia, et al., Diagnosis of breast cancer based on modern mammography using hybrid transfer learning, Multidimens Syst. Signal Process. 32 (2021) 747–765.

[6] P. Falagan-Lotsch, E.M. Grzincic, C.J. Murphy, New advances in nanotechnology-based diagnosis and therapeutics for breast cancer: an assessment of active-targeting inorganic nanoplatforms, Bioconjug. Chem. 28 (1) (2017) 135–152.

[7] Jurisic, V., S. Radenkovic, and G. Konjevic, The actual role of LDH as tumor marker, biochemical and clinical aspects. Advances in Cancer Biomarkers: From Biochemistry to Clinic For a Critical Revision, 2015: p. 115–124.

[8] S. Radenkovic, et al., HER2-positive breast cancer patients: correlation between mammographic and pathological findings, Radiat. Prot. Dosimetry 162 (1–2) (2014) 125–128.

[9] S. Radenkovic, et al., pSTAT3 expression associated with survival and mammographic density of breast cancer patients, Pathology-Res. Pract. 215 (2) (2019) 366–372.

[10] Q. Dang, et al., Fabrication and evaluation of thermosensitive chitosan/collagen/α, β-glycerophosphate hydrogels for tissue regeneration, Carbohydr. Polym. 167 (2017) 145–157.

[11] S. Thibodeau, I.A. Voutsadakis, FOLFIRINOX chemotherapy in metastatic pancreatic cancer: a systematic review and meta-analysis of retrospective and phase II studies, J. Clin. Med. 7 (1) (2018) 7.

[12] W. Yongnan, et al., Clinical value of the changes of ER,. PR,. HER2 and Ki? 郢 67 expressions before and after neoadjuvant chemotherapy in breast cancer, Lingnan Mod. Clin. Surg. 13 (04) (2023) 308.

[13] K. Ashtari, et al., A biotemplated nickel nanostructure: synthesis, characterization and antibacterial activity, Mater. Res. Bull. 50 (2014) 348–353.

[14] J.C. Antunes, et al., Drug targeting of inflammatory bowel diseases by biomolecules, Nanomaterials 11 (8) (2021) 2035.

[15] S. Yuvaraj, M.P. Peppelenbosch, N.A. Bos, Transgenic probiotica as drug delivery systems: the golden bullet? Expert. Opin. Drug Deliv. 4 (1) (2007) 1–3.

[16] S. Ranjbar, et al., Emerging roles of probiotics in prevention and treatment of breast cancer: a comprehensive review of their therapeutic potential, Nutr. Cancer 71 (1) (2019) 1–12.

[17] T. Didari, et al., A systematic review of the safety of probiotics, Expert Opin. Drug Saf. 13 (2) (2014) 227–239.

[18] M. Sharifi, et al., Kefir: a powerful probiotics with anticancer properties, Med. Oncol. 34 (11) (2017) 1–7.

[19] J. Roze, et al., *In vitro* systematic drug testing reveals carboplatin, paclitaxel, and alpelisib as a potential novel combination treatment for adult granulosa cell tumors, Cancers 13 (3) (2021) 368 (Basel).

[20] V. Gogvadze, S. Orrenius, B. Zhivotovsky, Mitochondria as targets for cancer chemotherapy. Seminars in Cancer Biology, Elsevier, 2009.

[21] P.J. Hung, et al., Continuous perfusion microfluidic cell culture array for high-throughput cell-based assays, Biotechnol. Bioeng. 89 (1) (2005) 1–8.

[22] M.-H. Wu, S.-.B. Huang, G.-.B. Lee, Microfluidic cell culture systems for drug research, Lab. Chip 10 (8) (2010) 939–956.

[23] Á. Dos Santos, et al., High-throughput mechanobiology: force modulation of ensemble biochemical and cell-based assays, Biophys. J. 120 (4) (2021) 631–641.

[24] S.A. Sundberg, High-throughput and ultra-high-throughput screening: solution-and cell-based approaches, Curr. Opin. Biotechnol. 11 (1) (2000) 47–53.

[25] A. Ramirez, et al., Microfluidic systems to study tissue barriers to immunotherapy, Drug Deliv. Transl. Res. (2021) 1–16.

[26] M.D. Bourn, et al., High-throughput microfluidics for evaluating microbubble enhanced delivery of cancer therapeutics in spheroid cultures, J. Controlled Release 326 (2020) 13–24.

[27] A. Ozcelikkale, et al., Differential response to doxorubicin in breast cancer subtypes simulated by a microfluidic tumor model, J. Controlled Release 266 (2017) 129–139.

[28] B. Subia, et al., Breast tumor-on-chip models: from disease modeling to personalized drug screening, J. Controlled Release (2021).

[29] K.E. Sung, et al., Understanding the impact of 2D and 3D fibroblast cultures on *in vitro* breast cancer models, PLoS One 8 (10) (2013) e76373.

[30] S.J. Trietsch, et al., Microfluidic titer plate for stratified 3D cell culture, Lab. Chip 13 (18) (2013) 3548–3554.

[31] H.L. Lanz, et al., Therapy response testing of breast cancer in a 3D high-throughput perfused microfluidic platform, BMC Cancer 17 (1) (2017) 1–11.

[32] A. Boussommier-Calleja, et al., Microfluidics: a new tool for modeling cancer–immune interactions, Trends Cancer 2 (1) (2016) 6–19.

[33] M. Mehling, S. Tay, Microfluidic cell culture, Curr. Opin. Biotechnol. 25 (2014) 95–102.

[34] A.Y. Shourabi, N. Kashaninejad, M.S. Saidi, An integrated microfluidic concentration gradient generator for mechanical stimulation and drug delivery, J. Sci. Adv. Mater. Dev. 6 (2) (2021) 280–290.

[35] S. Kim, H.J. Kim, N.L. Jeon, Biological applications of microfluidic gradient devices, Integr. Biol. 2 (11–12) (2010) 584–603.

[36] Z. Bagheri, et al., On-chip analysis of carbon dots effect on yeast replicative lifespan, Anal. Chim. Acta 1033 (2018) 119–127.

[37] T. Richmond, N. Tompkins, 3D microfluidics in PDMS: manufacturing with 3D molding, Microfluid Nanofluidics 25 (9) (2021) 1–7.

[38] W. Bu, et al., A low-cost, programmable, and multi-functional droplet printing system for low copy number SARS-CoV-2 digital PCR determination, Sens. Actuators B 348 (2021), 130678.

[39] JI, U., et al., (2023) River sediment transport modeling of ele river using computational fluid dynamics model of COMSOL multiphysics program.

[40] N.M. Aborehab, M.R. Elnagar, N.E. Waly, Gallic acid potentiates the apoptotic effect of paclitaxel and carboplatin via overexpression of Bax and P53 on the MCF-7 human breast cancer cell line, J. Biochem. Mol. Toxicol. 35 (2) (2021) e22638.

[41] X. Zhuang, et al., Novel lecithin-based oleogels and oleogel emulsions delay lipid oxidation and extend probiotic bacteria survival, LWT 136 (2021), 110353.

[42] M. Yoozbashi, et al., Magnetic nanostructured lipid carrier for dual triggered curcumin delivery: preparation, characterization and toxicity evaluation on isolated rat liver mitochondria, J. Biomater. Appl. (2021), 08853282211034625.

[43] S.J. Reinholt, H.G. Craighead, Microfluidic device for aptamer-based cancer cell capture and genetic mutation detection, Anal. Chem. 90 (4) (2018) 2601–2608.

[44] V. Jurisic, et al., TNF-α induced apoptosis is accompanied with rapid CD30 and slower CD45 shedding from K-562 cells, J. Membr. Biol. 239 (2011) 115–122.

[45] A.E. Milner, H. Wang, C.D. Gregory, Analysis of apoptosis by flow cytometry. Flow Cytometry Applications in Cell Culture, CRC Press, 2020, pp. 193–209.

[46] L. Yang, et al., Reactive oxygen species mediate anlotinib-induced apoptosis via activation of endoplasmic reticulum stress in pancreatic cancer, Cell Death. Dis. 11 (9) (2020) 1–15.

[47] D. An, K. Kim, J. Kim, Microfluidic system based high throughput drug screening system for curcumin/TRAIL combinational chemotherapy in human prostate cancer PC3 cells, Biomol. Ther. 22 (4) (2014) 355 (Seoul).

[48] Y. Choi, et al., A microengineered pathophysiological model of early-stage breast cancer, Lab. Chip, 15 (16) (2015) 3350–3357.

[49] A. Lamberti, S. Marasso, M. Cocuzza, PDMS membranes with tunable gas permeability for microfluidic applications, Rsc Adv. 4 (106) (2014) 61415–61419.

[50] J. Han, et al., Anti-proliferative and apoptotic effects of oleuropein and hydroxytyrosol on human breast cancer MCF-7 cells, Cytotechnology 59 (2009) 45–53.

[51] Z. Marcsek, et al., Effect of formaldehyde and resveratrol on the viability of Vero, HepG2 and MCF-7 cells, Cell Biol. Int. 31 (10) (2007) 1214–1219.

[52] K. Mukaddam, et al., Effect of a nanostructured titanium surface on gingival cell adhesion, viability and properties against P. gingivalis, Materials 14 (24) (2021) 7686 (Basel).

[53] A.d.M. de LeBlanc, et al., Effects of milk fermented by Lactobacillus helveticus R389 on a murine breast cancer model, Breast Cancer Res. 7 (4) (2005) 1–10.

[54] M. Thirabunyanon, P. Boonprasom, P. Niamsup, Probiotic potential of lactic acid bacteria isolated from fermented dairy milks on antiproliferation of colon cancer cells, Biotechnol. Lett. 31 (4) (2009) 571–576.

[55] Y. Vandenplas, et al., Efficacy and safety of APT198K for the treatment of infantile colic: a pilot study, J. Comp. Eff. Res. 6 (2) (2017) 137–144.

[56] D.M. Kich, et al., Probiotic: effectiveness nutrition in cancer treatment and prevention, Nutr. Hosp. 33 (6) (2016) 1430–1437.

[57] Y.H. Chen, et al., Probiotic Lactobacillus spp. act against Helicobacter pylori-induced inflammation, J. Clin. Med. 8 (1) (2019) 90.

[58] C.V. De Almeida, et al., Differential responses of colorectal cancer cell lines to Enterococcus faecalis' strains isolated from healthy donors and colorectal cancer patients, J. Clin. Med. 8 (3) (2019) 388.

[59] L. Zorzela, et al., Is there a role for modified probiotics as beneficial microbes: a systematic review of the literature, Benef. Microbes 8 (5) (2017) 739–754.

[60] J.S. Schwartz, et al., Topical probiotics as a therapeutic alternative for chronic rhinosinusitis: a preclinical proof of concept, Am. J. Rhinol. Allergy 30 (6) (2016) e202–e205.

[61] S.H. Lee, et al., Therapeutic effect of tyndallized Lactobacillus rhamnosus IDCC 3201 on atopic dermatitis mediated by down-regulation of Immunoglobulin E in NC/Nga Mice, Microbiol. Immunol. 60 (7) (2016) 468–476.

[62] N. Piqué, M. Berlanga, D. Miñana-Galbis, Health benefits of heat-killed (Tyndallized) probiotics: an overview, Int. J. Mol. Sci. 20 (10) (2019) 2534.

[63] Ş. Comşa, A.M. Cimpean, M. Raica, The story of MCF-7 breast cancer cell line: 40 years of experience in research, Anticancer Res. 35 (6) (2015) 3147–3154.

[64] S. Amiri, et al., Clozapine attenuates mitochondrial dysfunction, inflammatory gene expression, and behavioral abnormalities in an animal model of schizophrenia, Neuropharmacology 187 (2021), 108503.

[65] P. Fathi, et al., Effects of copper oxide nanoparticles on the Chlorella algae in the presence of humic acid, SN Appl. Sci. 2 (2) (2020) 1–11.

[66] A.C. Martínez-Torres, et al., Chitosan gold nanoparticles induce cell death in HeLa and MCF-7 cells through reactive oxygen species production, Int. J. Nanomed. (2018) 3235–3250.

[67] B. Lei, et al., Low-concentration BPAF-and BPF-induced cell biological effects are mediated by ROS in MCF-7 breast cancer cells, Environ. Sci. Pollut. Res. 25 (2018) 3200–3208.

[68] S. Paul, et al., Stevioside induced ROS-mediated apoptosis through mitochondrial pathway in human breast cancer cell line MCF-7, Nutr. Cancer 64 (7) (2012) 1087–1094.

[69] P. Naserzadeh, et al., Biocompatibility assessment of titanium dioxide nanoparticles in mice fetoplacental unit, J. Biomed. Mater. Res. Part A 106 (2) (2018) 580–589.

[70] A.S.B. Ershadi, et al., SAHA improves depressive symptoms, cognitive impairment and oxidative stress: rise of a new antidepressant class, Neurochem. Res. 46 (5) (2021) 1252–1263.

[71] N. Engel, et al., Pro-apoptotic and anti-adhesive effects of four African plant extracts on the breast cancer cell line MCF-7, BMC Complement. Altern. Med. 14 (2014) 1–13.

[72] S. Kaushik, et al., Dietary isoflavone daidzein synergizes centchroman action via induction of apoptosis and inhibition of PI3K/Akt pathway in MCF-7/MDA MB-231 human breast cancer cells, Phytomedicine 40 (2018) 116–124.

[73] A. Mari, et al., Carvacrol promotes cell cycle arrest and apoptosis through PI3K/AKT signaling pathway in MCF-7 breast cancer cells, Chin. J. Integr. Med. 27 (2021) 680–687.

[74] C.G. Yedjou, E.B. Izevbigie, P.B. Tchounwou, Vernonia amygdalina—Induced growth arrest and apoptosis of breast cancer (MCF-7) cells, Pharmacol. Pharm. 4 (1) (2013).